ISSN: 0256-307X

中国物理快报

Chinese Physics Letters

Volume 31 Number 10 October 2014

A Series Journal of the Chinese Physical Society
Distributed by IOP Publishing

Online: http://iopscience.iop.org/0256-307X
http://cpl.iphy.ac.cn

TRUST FOR AUTHORS
— CHINESE PHYSICS LETTERS

CHINESE PHYSICAL SOCIETY
IOP Publishing

CHIN. PHYS. LETT. Vol. 31, No. 10 (2014) 104203

High-Power High-Efficiency Laser Power Transmission at 100 m Using Optimized Multi-Cell GaAs Converter *

HE Tao(何滔)[1], YANG Su-Hui(杨苏辉)[1**], Miguel Ángel Muñoz[2], ZHANG Hai-Yang(张海洋)[1], ZHAO Chang-Ming(赵长明)[1], ZHANG Yi-Chen(张逸辰)[1], XU Peng(徐鹏)[1]

[1]*School of Optoelectronics, Beijing Institute of Technology, Beijing 100081*
[2]*Physical Properties Laboratory, Technical University of Madrid, Madrid 28040, Spain*

(Received 24 April 2014)

A high-power high-efficiency laser power transmission system at 100 m based on an optimized multi-cell GaAs converter capable of supplying 9.7 W of electricity is demonstrated. An I–V testing system integrated with a data acquisition circuit and an analysis software is designed to measure the efficiency and the I–V characteristics of the laser power converter (LPC). The dependencies of the converter's efficiency with respect to wavelength, laser intensity and temperature are analyzed. A diode laser with 793 nm of wavelength and 24 W of power is used to test the LPC and the software. The maximum efficiency of the LPC is 48.4% at an input laser power of 8 W at room temperature. When the input laser power is 24 W (laser intensity of 60000 W/m^2), the efficiency is 40.4% and the output voltage is 4 V. The overall efficiency from electricity to electricity is 11.6%.

PACS: 42.15.Eq, 42.68.Ay, 72.40.+w, 84.60.Jt DOI: 10.1088/0256-307X/31/10/104203

Laser power transmission provides a powering link insensitive to electromagnetic noise and electrically isolated between the ends.[1,2] Laser power can be effectively converted into electricity by appropriate photovoltaic (PV) cells based on semiconductor heterostructure. Many experiments involving laser power transmission technology have been reported. In 1997, Yugami *et al.* tested a GaAs cell (4 cm^2 area) with a laser at a wavelength of 808 nm and power of 1 W. The laser power intensity was 2500 W/m^2. The conversion efficiency of the GaAs cell they obtained was 51%, while the fill factor was not considered.[3] In 2002, Steinsiek *et al.* transmitted a 5 W laser ($\lambda = 532$ nm) to drive a small rover vehicle over a distance of 280 m. The rover was equipped with InGaP cells (18.9 cm^2 area); the efficiency of the InGaP cells was 40% under an intensity of 2648 W/m^2.[4] However, few data have been published on the performance of converters at higher laser power intensity. Due to the fact that when a PV cell is illuminated under high laser intensity, the thermal effect will cause an increase of series resistance of the cell,[5–7] therefore, the efficiency of a PV cell drops with the higher laser intensity. In 2012, Mukherjee *et al.* demonstrated an InGaAs/InP converter (0.25 cm^2 area) illuminated by a laser ($\lambda = 1.55$ μm) with a conversion efficiency of 44.6% under an illumination intensity of 1000 W/m^2; however, the efficiency dropped to 40.6% when the illumination intensity was boosted to 2370 W/m^2.[8]

In some applications, converters working at high laser power and intensity are more desirable to reduce the volume and cost of whole systems. Therefore, one of the research topics in this area is how to improve the conversion efficiency from laser power to electricity at high laser illuminating power and intensity. In this Letter, a specially designed optimized multi-cell GaAs converter working at high laser intensity is presented. We demonstrate a high power space laser transmission system capable of supplying 9.7 W electricity. A 793 nm diode laser at a distance of 100 m is used to illuminate the optimized multi-cell GaAs converter, the maximum efficiency of the LPC from laser power to electricity is 48.4% at an input laser power of 8 W (20000 W/m^2) at room temperature. Moreover, the efficiency is 40.4% when the laser power is 24 W (60000 W/m^2). The overall efficiency (the product of the laser wall-plug efficiency, the optical system's transmission efficiency and the LPC conversion efficiency) from electricity to electricity is 11.6%. Compared with the previous works,[9] the transmission system is improved dramatically with the longer transmission distance, higher laser power and greater electricity supply. A newly designed *I–V* testing system is used to measure the performance of the GaAs converter.

A laser power transmission system with parameters shown in Fig. 1 is designed to transmit a laser to an LPC. A fiber coupled laser diode at 793 nm is selected. Its wavelength is close to the absorption peak of the GaAs cell. A telescope is installed on a three-dimensional electric motor platform for automatically tracking the LPC, as shown in Fig. 2(a). To reduce chromatic aberration, an aspherical lens is used as the collimating lens. Its parameters are optimized with the ZEMAX software. A receiving lens is used to focus the laser beam on to the LPC, as shown in

*Supported by the National High-Technology Research and Development Program of China under Grant 2012AA120605.
**Corresponding author. Email: suhuiyang@bit.edu.cn
© 2014 Chinese Physical Society and IOP Publishing Ltd

TOP AUTHORS — CHINESE PHYSICS LETTERS

Fig. 2(b). We measured the laser power at the position of the LPC; the transmittances of the optics at different emitted laser powers are presented in Table 1. An I–V test system is integrated with a data acquisition circuit, analysis software and a display.

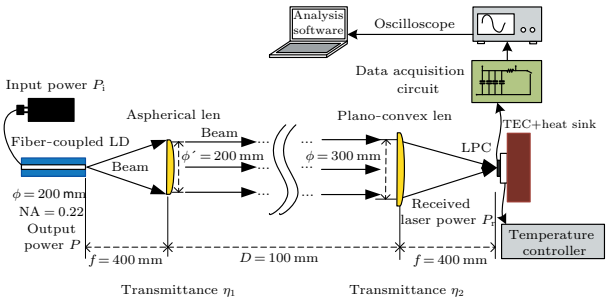

Fig. 1. Schematic diagram of the laser power transmission at 100 m and the data analysis system.

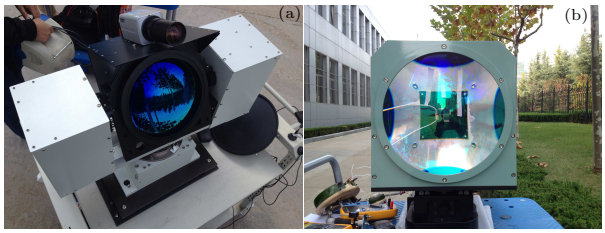

Fig. 2. Photographs of the automatic tracking telescope system and receiving system.

Table 1. Transmittance of the 100 m transmission optical system.

Emitted laser power (W)	11.80	25.00	39.80	52.70
Received laser power (W)	10.90	24.00	38.30	51.40
Transmission efficiency (%)	92.3	96	96.2	97.5

To make an electron free in the material from its covalent bond, the energy of the photon needs to be higher than the 'band-gap energy' of the material. Band-gap energy E_g is inversely proportional to the cutoff wavelength λ_c,

$$\lambda_c = 1240/E_g, \tag{1}$$

where E_g is in electron volts and λ_c is in nanometers.

The band-gap energy E_g can be commonly expressed in terms of α and β coefficients of the Varshni equation

$$E_g(T) = E_g(0) - \frac{\alpha T^2}{T+\beta}, \tag{2}$$

where $E_g(0)$ is the band-gap energy at 0 K, α is in electron volts per degree Kelvin, and β is proportional to the Debye temperature (in Kelvin). For GaAs $E_g(0) = 1.517$, $\alpha = 5.5$, $\beta = 225$.[10] Substitute these values into Eq. (2), we can calculate the band-gap energy at different temperatures. At room temperature 298 K, E_g is 1.424 eV. According to Eq. (1), the cutoff wavelength is calculated to be $\lambda_c = 870$ nm.

The spot diameter of the transmitted laser beam is given by

$$\phi_{spot} = 2.44\lambda D/\phi', \tag{3}$$

where ϕ' is the diameter of the optics for collimation, and D is the transmission distance.

Figure 3(a) shows the single-junction GaAs structure on a Germanium substrate. The thickness of each layer was optimized for working at high laser intensity. It consists of: the n-Ge substrate (175 μm), n-GaAs buffer (0.5 μm), n-AlGaAs BSF (100 nm), n-GaAs baser (3 μm), p-GaAs emitter (400 nm), p-InGaP window (50 nm), and p^{++}-GaAs cap layer (0.5 μm). The GaAs cell has a photosensitive surface area of $10 \times 10\,\text{mm}^2$. This structure is optimized for operation at more than $50000\,\text{W/m}^2$ laser intensity. The cell's surface is coated with antireflective coating (TiO_x/SiO_2) for the 400–900 nm wavelength. Figure 3(b) is the top view of a single cell mounted on a copper substrate with n-side down. Four such cells are connected in a series from a monolithic block, as shown in Fig. 3(c). The photosensitive surface area is $400\,\text{mm}^2$. Here 1 mm gaps remained between cells for electrode connection. Figure 3(d) shows the LPC consisting of an optics, a monolithic block, a thermoelectric cooler and a heat sink.[11]

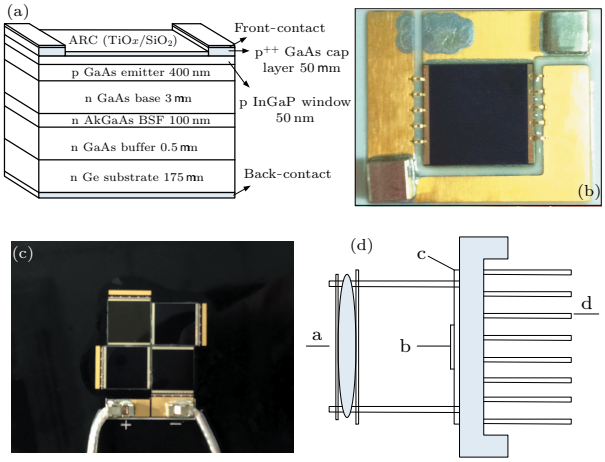

Fig. 3. (a) A GaAs cell fabricated on a Ge substrate. (b) Top view of the prototype of a single GaAs cell with a photosensitive surface area of $10 \times 10\,\text{mm}^2$. (c) Optimized multi-cell GaAs cells with a photosensitive surface area of $20 \times 20\,\text{mm}^2$. (d) Schematic diagram of the laser power converter: a–optics, b–monolithic block, c–thermoelectric cooler, and d–heat sink.

Under high intensity laser illumination, the process of measuring a GaAs cell's output characteristics is critical due to the fact that a GaAs cell has low open-circuit voltage and high short-circuit current. Presently, the methods for measuring the I–V curve can be divided into passive load and active load. Passive load can be resistive or capacitive. With a capacitive load, one can reach almost the short circuit current, the only limit is the internal series resistance.

TOP AUTHORS — Chinese Physics Letters

This makes using a capacitive load a better solution for measuring I–V characteristics. Figure 4 shows the schematic diagram of the I–V testing circuit with a capacitive load. Test points 1 and 2 are connected to an oscilloscope with two channels to measure the current and voltage slopes respectively. The value of the shunt resistor must be small and precise enough to meet the load capacity of the cell. For testing a single cell, we choose 0.1 Ω value of the shunt resistor, its precision is 1%. For testing the optimized multi-cell GaAs cells, another resistor with a value of 1.5 Ω is used. The capacitor must be large enough to offer a long charging time. The value of the capacitor is 470 μF (KEMET, P/N: T520D477M004ATE010), the parasite equivalent series resistance (ESR) is 10 mΩ. Note that the ESR of each capacitor can greatly affect the testing data due to the drop of voltage on it, thus several capacitors are connected in parallel to reduce the ESR. The I–V data are obtained by an oscilloscope and transferred to a computer with an analysis software designed with Labview . The software integrates functions of the I–V curve record, max power point finding and fill factor calculation.

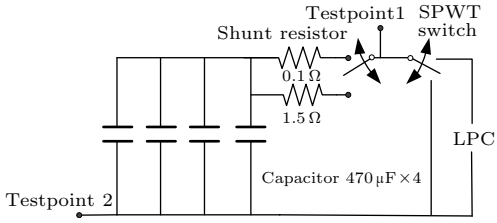

Fig. 4. Schematic diagram of the I–V test system with capacitive load.

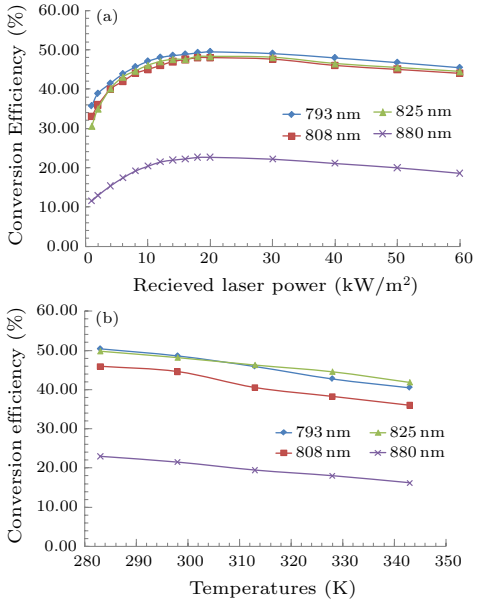

Fig. 5. GaAs response with respect to wavelengths, laser intensity and temperatures.

A single GaAs cell, shown in Fig. 2(b), is tested indoors to analyze the dependencies of the single GaAs efficiency with respect to wavelength, laser intensity and temperature. We tested laser diodes at wavelengths of 793 nm, 808 nm, 825 nm and 880 nm. Figure 5(a) shows the dependency of efficiency with respect to laser intensity; it is shown that, at low intensity, the efficiency increases slightly with the laser intensity and gradually becomes saturated, when the laser intensity is higher than 20000 W/m^2, the efficiency declines due to the increase of the series resistance of the cell; the highest efficiency of 49.7% is obtained when the laser intensity is 20000 W/m^2 at $\lambda = 793$ nm. To the best of our knowledge, this is the highest conversion efficiency obtained at such high laser intensity. The efficiency is much lower at $\lambda = 880$ nm due to the fact that the photon energy is lower than the GaAs material band gap. The efficiency decreases with the increase of temperature, as shown in Fig. 5(b).

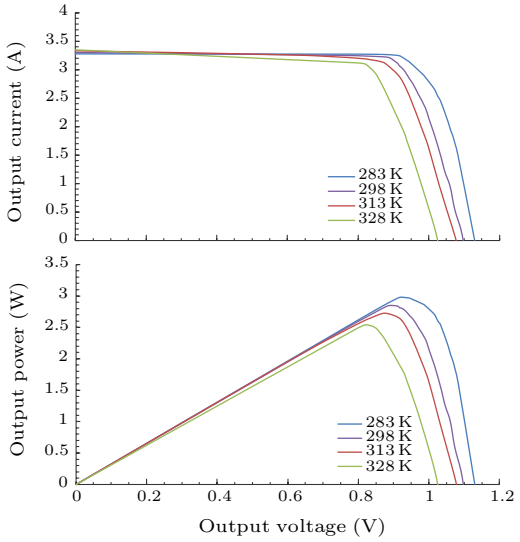

Fig. 6. The I–V and power-voltage curves.

As shown in Fig. 5(b), the conversion efficiency decreases with the increase of temperature. The dependency of the efficiency η to temperature T is expressed by

$$\eta(T) = \eta(298\,\mathrm{K}) + \frac{\eta(298\,\mathrm{K})(T - 298\,\mathrm{K})}{\eta}\frac{d\eta}{dT}, \tag{4}$$

where $(d\eta/dT)/\eta$ is the normalized temperature coefficient of the efficiency. Note that η is related to the cell's maximum power P_m. Clearly, $(d\eta/dT)/\eta = (dP_\mathrm{m}/dT)/P_\mathrm{m}$. The temperature coefficient is determined by the variation of open voltage, short current and fill factor using the relation

$$\frac{1}{P_\mathrm{m}}\frac{dP_\mathrm{m}}{dT} = \frac{1}{I_\mathrm{sc}}\frac{dI_\mathrm{sc}}{dT} + \frac{1}{U_\mathrm{oc}}\frac{dU_\mathrm{oc}}{dT} + \frac{1}{FF}\frac{dFF}{dT}, \tag{5}$$

where P_m is the cell's maximum power, I_sc is the short circuit current, U_oc is the open circuit voltage,

TOP-TIER ARTICLES — CHINESE PHYSICS LETTERS

and FF is the fill factor of the cell. For monochromatic illumination, the change in short circuit current I_{sc} and FF is negligible. Thus the temperature efficiency coefficient is mainly determined by the variation of open circuit voltage U_{oc}. Here $1/\eta(d\eta/dT) = 1/U_{oc}(dU_{oc}/dT)$, the temperature coefficient of open voltage

$$\frac{dU_{oc}}{dT} = \frac{U_{oc} - E_g(T)}{T} - \frac{3k}{q} - \frac{\alpha T(T+2\beta)}{(T+\beta)^2}. \quad (6)$$

It is observed that the temperature coefficient of open voltage is negative.[12] Combining with Eq. (4), as the temperature coefficient is negative, it is seen that the efficiency decreases with the increase of temperature.

Figure 6 shows the GaAs cell response curve illuminated at $\lambda = 793$ nm laser intensity of 60000 W/m^2 with different temperatures.

Figure 6(a) shows the I–V curves at the temperatures of 283 K, 298 K, 313 K, and 328 K. Here U_{oc} increases logarithmically with the short circuit current I_{sc}, and U_{oc} decreases with the increase of temperature.[13–15]

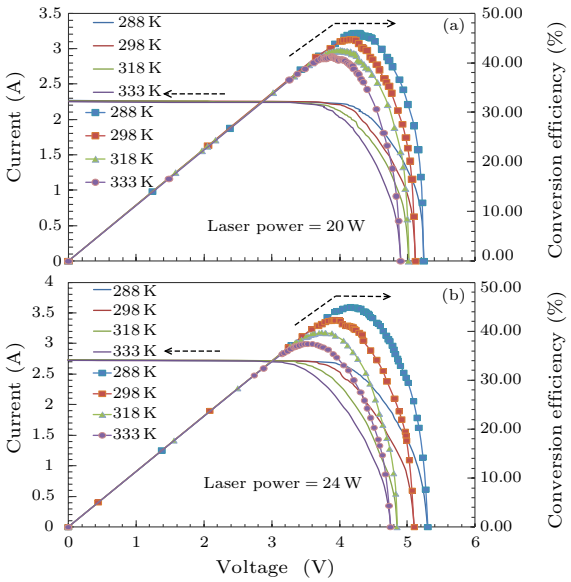

Fig. 7. The I–V curve and efficiency-voltage curve under 20 W and 24 W laser illumination for the optimized multi-cell LPC.

Graphically, the fill factor is a measure of the 'squareness' of the I–V curve and is the area of the largest rectangle that fits in the I–V curve. The fill factor is also defined as the ratio of maximum obtainable power to the product of the open-circuit voltage U_{oc} and short-circuits current I_{sc}.[16] The expression is

$$\mathrm{FF} = U_{max} I_{max} / U_{oc} I_{sc}, \quad (7)$$

where U_{max} and I_{max} are the voltage and current at the maximum power point. The maximum power point is displayed as the vertex of the power-voltage curve in Fig. 6(b), which reveals that the maximum power descends with the increase of temperature. Apparently, it is seen that the cell fill factor decreases with the increase of temperature.

The LPC with optimized multi-cell GaAs cells is tested in a 100 m laser power transmission outdoor experiment. Figure 7 shows the LPC response curve illuminated by laser powers of 20 W (a) and 24 W (b) at different temperatures. Note that the curves with marks are the efficiency-voltage curves, the others are the I–V curves. Apparently, both the cell fill factor and the open circuit voltage decrease with the increase of temperature.

In the case of natural cooling, where the thermoelectric cooler of the LPC is switched off, we measure the dependencies of the temperature and efficiency of the LPC with respect to time. The initial environmental temperature is 26.4℃. Figure 8 shows the temperature increases logarithmically over time, while the efficiency decreases rapidly after 5 min exposure. After 1 h, the temperatures (efficiency) stabilize at 65.0℃ (35.6%), 59.3℃ (37.7%) and 52.7℃ (40.9%) when the LPC is illuminated at laser powers of 24 W, 20 W and 16 W, respectively.

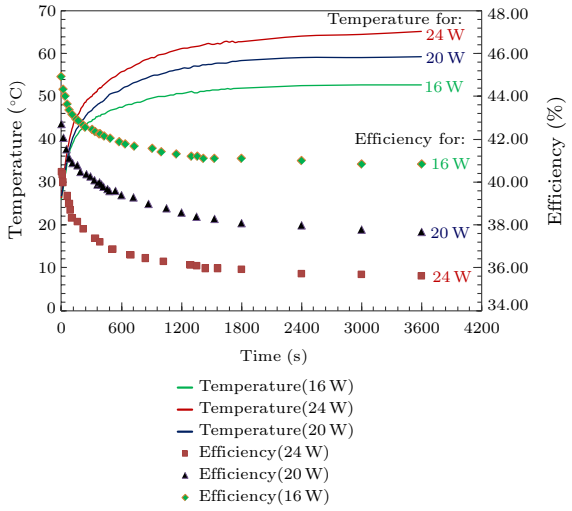

Fig. 8. Temperature and efficiency versus time.

When the temperature is fixed at 25℃, the LPC conversion efficiencies illuminated at different laser powers are shown in Table 2. The LPC is capable of supplying 9.7 W of electricity at 24 W laser illumination with a high efficiency of 40.4%.

To analyze the overall efficiency of the laser power transmission system, the temperature is fixed at room temperature 298 K. The cell's maximum power is 9.7 W. The voltage is 4 V and the current is 2.43 A with FF of 80%. The laser wall-plug efficiency is 30% measured at an emitted laser power of 25 W. The test transmittance of the optical system is 96% (shown in Table 1) for a 793 nm laser. The atmospheric transmission loss can be ignored due to the relatively short

JUST FOR AUTHORS — CHINESE PHYSICS LETTERS

transmission distance. The received laser power measured at the position of cell is 24 W. Here the data of the energy used to cool the cell is not included. In result, when the laser intensity is 60000 W/m^2 and the GaAs optical-electrical conversion efficiency is 40.4%, the overall efficiency (the product of the laser wall-plug efficiency, the optical system's transmission efficiency and LPC conversion efficiency) is 11.6%.

Table 2. LPC conversion efficiency at different laser powers (25℃).

Laser power (W)	2	4	8	12	16	20	24
Efficiency (%)	35.0	44.5	48.4	47.0	44.9	42.7	40.4

In summary, a high power laser transmission system at a distance of 100 m is demonstrated. An LPC with an optimized multi-cell GaAs converter capable of supplying 9.7 W of electricity at 24 W laser illumination with a high efficiency of 40.4% is fabricated. The overall efficiency from electricity to electricity is 11.6%. The dependencies of the converter's efficiency with respect to wavelength, laser power and temperature are measured and analyzed. Compared with the previous work in laser power transmission technology, we obtain a relatively high efficiency under high laser power and intensity. Such a laser power transmission system could prove to be extremely useful as a future power source, specifically in regions and targets where conventional energy delivery systems are disabled.

The authors thank the group of Shi Dele in the Shandong Institute of Aerospace Electronics for the design of the automatic tracking mechanical platform.

References

[1] Peña R and Algora C 2001 *IEEE Trans. Electron Devices* **48** 196
[2] Peña R and Algora C 2012 *Prog. Photovolt.: Res. Appl.* **20** 117
[3] Yugami H, Kanamori Y, Arashi H, Niino M, Moro A, Eguchi K, Okada Y and Endo A 1997 *Proc. IEEE Conf. Energy Conversion Engineering* (Honolulu HI 1997) p 625
[4] Steinsiek F, Foth W P, Weber K H, Foth H J and Schäfer C 2003 *Proc. 54th International Astronautical Congress* (Bremen, Germany 2003) p 169
[5] Katz E A, Gordon J M, Tassew W and Feuermann D 2006 *Appl. Phys.* **100** 044514
[6] Gerard J B, Peter M, Erik J H, John J S, Nash L J, Dominic J F F, Ian M B and Geoffrey D 2010 *Proc. 6th International AIP Conf. on Concentrating Photovoltaic Aystems: CPV-6* (Freiburg, Germany 2010) p 16
[7] Algora C, Ortiz E, Stolle I R, Diaz V, Peña R, Andreev V M, Khvostikov V P and Rumyantsev V D 2001 *IEEE Trans. Electron Devices* **48** 840
[8] Mukherjee J, Jarvis S, Perren M and Sweeney S J 2013 *J. Phys. D: Appl. Phys.* **46** 264006
[9] He T, Yang S H, Zhang H Y, Zhao C M, Xu P, Hao J Y and Wang H X 2013 *Chin. J. Lasers* **40** 0317001
[10] Lautenschlager P, Garriga M, Logothetidis S and Caedona M 1987 *Phys. Rev.* B **35** 9174
[11] Cui M, Chen N F, Deng J X and Liu L Y 2013 *Chin. Phys.* B **22** 84208
[12] Fan J C C 1986 *Sol. Cells* **17** 309
[13] Yang C C, Jang C H, Sheu J K, Lee M L, Tu S L, Huang F W, Yeh Y H and Lai W C 2011 *Opt. Express* **19** A695
[14] Zhang D Y, Zheng X H, Li X F, Wu Y Y, Wang J F and Yang H 2012 *Chin. Phys. Lett.* **29** 068801
[15] Mathews I, O'Mahony D, Corbett B and Morrison A P 2012 *Opt. Express* **20** A754
[16] Zhang W, Chen C, Jia R, Janssen G J M, Zhang D S, Xing Z, Bronsveld P C P, Weeber A W, Jin Z and Liu X Y 2013 *Chin. Phys. Lett.* **30** 078801

JUST FOR AUTHORS — CHINESE PHYSICS LETTERS

Chinese Physics Letters

Volume 31 Number 10 October 2014

GENERAL

100301 Selective Tunneling Dynamics of Bosons with Effective Three-Particle Interactions
NIU Zhen-Xia, XUE Ju-Kui

100401 Spontaneous Emission of a Two-Level Static Atom Coupling with Electromagnetic Vacuum Fluctuations Outside a High-Dimensional Einstein Gauss-Bonnet Black Hole
ZHANG Ming, YANG Zhan-Ying, YUE Rui-Hong

100501 Paths to Synchronization on Complex Networks with External Drive
ZOU Ying-Ying, LI Hai-Hong

100502 The Heisenberg Model after an Interaction Quench
ZHOU Zong-Li, LI Min, YE Jian, LI Dong-Peng, LOU Ping, ZHANG Guo-Shun

100601 Accurate Evaluation of Microwave-Leakage-Induced Frequency Shifts in Fountain Clocks
FANG Fang, LIU Kun, CHEN Wei-Liang, LIU Nian-Feng, SUO Rui, LI Tian-Chun

100702 Mechanism and Simulation of Generating Pulsed Strong Magnetic Field
YANG Xian-Jun, WANG Shuai-Chuang, DENG Ai-Dong, GU Zhuo-Wei, LUO Hao

NUCLEAR PHYSICS

102101 Simulation and Characterization of Aluminium Three-Dimensional Resonator for Quantum Computation
ZHAO Hu, LI Tie-Fu, LIU Qi-Chun, LIU Jian-She, CHEN Wei

102102 Tensor Force Effect on Shape Coexistence of $N = 28$ Neutron-Rich Isotones
WANG Yan-Zhao, GU Jian-Zhong, YU Guo-Liang, HOU Zhao-Yu

102401 Geometric Scaling in New Combined Hadron-Electron Ring Accelerator Data
ZHOU Xiao-Jiao, QI Lian, KANG Lin, ZHOU Dai-Cui, XIANG Wen-Chang

102501 Nucleon Emission Number as a Probe of Isospin-Dependent N–N Cross Section in Photonuclear Reactions
GUO Wen-Jun, HUANG Jiang-Wei, YONG Gao-Chan, ZHANG Xiao-Ji, ZHANG Ao

ATOMIC AND MOLECULAR PHYSICS

103201 Polarization Transfer in the $2p_{3/2}$ Photoionization of Magnesium-Like Ions
MA Kun, DONG Chen-Zhong, XIE Lu-You, QU Yi-Zhi

103202 Electron Dynamics of Atoms in Parallel Electric and Magnetic Fields
YANG Hai-Feng, GAO Wei, CHENG Hong, LIU Hong-Ping

103203 Determination of Atomic Number Densities of ^{87}Rb and ^{3}He Based on Absorption Spectroscopy
ZHENG Hui-Jie, QUAN Wei, LIU Xiang, CHEN Yao, LU Ji-Xi

FUNDAMENTAL AREAS OF PHENOMENOLOGY(INCLUDING APPLICATIONS)

104201 High-Precision Two-Dimensional Atom Localization in a Cascade-Type Atomic System
CHEN Jing-Dong, FANG Yu-Hong, ZHANG Ting

104202 Contributions of the Two Nuclei to the Harmonic Generation in H_2^+ Molecules
PEI Ya-Nan, MIAO Xiang-Yang

104203 High-Power High-Efficiency Laser Power Transmission at 100 m Using Optimized Multi-Cell GaAs Converter
HE Tao, YANG Su-Hui, Miguel Ángel Muñoz, ZHANG Hai-Yang, ZHAO Chang-Ming, ZHANG Yi-Chen, XU Peng

JUST FOR AUTHORS — CHINESE PHYSICS LETTERS

104301 Optimization of the Monopole Acoustic Transducer for Logging-while-Drilling
FU Lin, WANG Dong, WANG Xiu-Ming

104302 Guided Wave Propagation in a Gold Electrode Film on a $Pb(Mg_{1/3}Nb_{2/3})O_3$–33%$PbTiO_3$ Ferroelectric Single Crystal Substrate
HUANG Nai-Xing, LÜ Tian-Quan, ZHANG Rui, WANG Yu-Ling, CAO Wen-Wu

PHYSICS OF GASES, PLASMAS, AND ELECTRIC DISCHARGES

105201 Repetitive 'Snakes' and Their Damping Effect on Core Toroidal Rotation in EAST Plasmas with Multiple H–L–H Transitions
XU Li-Qing, HU Li-Qun, CHEN Kai-Yun, LI Chang-Zheng, LI Er-Zhong, ZHAO Jin-Long, SHENG Xiu-Li, ZHANG Ji-Zong, MAO Song-Tao

105202 Mode Transition of Vacuum Arc Discharge and Its Effect on Ion Current
LAN Chao-Hui, LONG Ji-Dong, ZHENG Le, PENG Yu-Fei, LI Jie, YANG Zhen, DONG Pan

CONDENSED MATTER: STRUCTURE, MECHANICAL AND THERMAL PROPERTIES

106101 Chemical Composition Dependent Elastic Strain in AlGaN Epilayers
WANG Huan, YAO Shu-De

106102 Effect of Indium and Antimony Doping on SnS Photoelectrochemical Solar Cells
Sunil H. Chaki, Mahesh D. Chaudhary, M. P. Deshpande

106103 Equivalent Trap Energy Level Extraction for SiGe Using Gate-Induced-Drain-Leakage Current Analysis
LIU Chang, YU Wen-Jie, ZHANG Bo, XUE Zhong-Ying, WU Wang-Ran, ZHAO Yi, ZHAO Qing-Tai

106201 Effective Dielectric Properties of Au-ZnS and Au-ZnO Plasmonics Nanocomposites in the Terahertz Regime
A. Zolanvar, H. Sadeghi, A. Ranjgar

106301 Mechanical and Vibrational Properties of ZnS with Wurtzite Structure: A First-Principles Study
YU You, CHEN Chun-Lin, ZHAO Guo-Dong, ZHENG Xiao-Lin, ZHU Xing-Hua

106401 A Kinetic Transition from Low to High Fragility in Cu-Zr Liquids
BI Qing-Ling, LÜ Yong-Jun

106801 A Source for the Excellent Floating Ability of a Water Strider
LIU Shuang, LIU Zhan-Wei, SHI Wen-Xiong

CONDENSED MATTER: ELECTRONIC STRUCTURE, ELECTRICAL, MAGNETIC, AND OPTICAL PROPERTIES

107301 The Effect of the Semiconductive Screen on Space Charge Suppression in Cross-Linked Polyethylene
LI Lin, HAN Bai, SONG Wei, WANG Xuan, LEI Qing-Quan

107302 Perfect Spin-Filtering in 4H-TAHDI-Based Molecular Devices: the Effect of N-Substitution
WU Qiu-Hua, ZHAO Peng, LIU De-Sheng

107303 A Forming-Free Bipolar Resistive Switching in HfO_x-Based Memory with a Thin Ti Cap
PANG Hua, DENG Ning

107304 Enhanced Current Carrying Capability of Au-ZnSe Nanowire-Au Nanostructure via High Energy Electron Irradiation
TAN Yu, WANG Yan-Guo

107501 Magnetic and Ferroelectric Properties of $BiCrO_3$ from First-Principles Calculations
DING Jun, KANG Xiu-Bao, WEN Li-Wei, LI Hai-Dong, ZHANG Jian-Min

107701 Local Piezoresponse and Thermal Behavior of Ferroelastic Domains in Multiferroic $BiFeO_3$ Thin Films by Scanning Piezo-Thermal Microscopy
YU Hui-Zhu, CHEN Hong-Guang, XU Kun-Qi, ZHAO Kun-Yu, ZENG Hua-Rong, LI Guo-Rong

JUST FOR AUTHORS
— CHINESE PHYSICS LETTERS

CROSS-DISCIPLINARY PHYSICS AND RELATED AREAS OF SCIENCE AND TECHNOLOGY

108401 A C-Band Internally-Matched High Efficiency GaN Power Amplifier
MA Xiao-Hua, WEI Jia-Xing, CAO Meng-Yi, LU Yang, ZHAO Bo-Chao, DONG Liang, WANG Yi, HAO Yue

108501 High-Pressure Water-Vapor Annealing for Enhancement of a-Si:H Film Passivation of Silicon Surface
GUO Chun-Lin, WANG Lei, ZHANG Yan-Rong, ZHOU Hai-Feng, LIANG Feng, YANG Zhen-Hui, YANG De-Ren

108502 Optical Performance of N-Face AlGaN Ultraviolet Light Emitting Diodes
YU Hong-Ping, LI Shi-Bin, ZHANG Peng, WU Shuang-Hong, WEI Xiong-Bang, WU Zhi-Ming, CHEN Zhi

108503 High Performance Long Wavelength Superlattice Photodetectors Based on Be Doped Absorber Region
ZHOU Yi, CHEN Jian-Xin, XU Zhi-Cheng, WANG Fang-Fang, XU Qing-Qing, XU Jia-Jia, BAI Zhi-Zhong, JIN Chuan, HE Li

108504 Non-Volatile Threshold Adaptive Transistors with Embedded RRAM
DEND Ning, JIA Hong-Yang, WU Wei, WU Hua-Qiang

108505 Junctionless Coplanar-Gate Oxide-Based Thin-Film Transistors Gated by Al_2O_3 Proton Conducting Films on Paper Substrates
WU Guo-Dong, ZHANG Jin, WAN Xiang

JUST FOR AUTHORS
— CHINESE PHYSICS LETTERS